ECASIA special issue paper

SURFACE and INTERFACE ANALYSIS

Received: 30 August 2013 Revised: 10 February 2014 Accepted: 17 February 2014 Published online in Wiley Online Library: 21 March 2014

(wileyonlinelibrary.com) DOI 10.1002/sia.5476

Gamma-irradiated silica sol–gel coatings as a function of dose on AA2024-T3†

A. Covelo,[a] A. Barba,[b] E. Bucio,[c] A. Tejeda[d] and M. Hernandez[b]*

The present paper reports the behavior of gamma-irradiated hybrid sol–gel coatings based on the copolymerization of 3-glycydoxypropyltrimethoxysilane and tetra-n-propoxyzirconium applied onto aluminum alloy AA2024-T3. Doses from 1 to 100 kGy were applied on undoped sol–gel coatings and coatings doped with hydrotalcite at 1% and 5%, *w/w*. The sol–gel coatings were deposited by using the dip-coating method on an aluminum substrate with a final grinding of a 240-grit. Scanning electron microscopy revealed that the hydrotalcite particles were heterogeneously dispersed at several micrometers in length. High irradiation doses on doped hydrotalcite coatings showed no improvement in the corrosion resistance of the films at longer immersion times in saline media obtained by electrochemical impedance spectroscopy. Differential scanning calorimetry showed that the gamma-irradiated doses and the hydrotalcite content modify the thermal properties of the sol–gel coatings. X-ray diffraction results revealed modification of the hydrotalcite crystallite size as a function of irradiation dose. Copyright © 2014 John Wiley & Sons, Ltd.

Keywords: EIS; sol–gel; irradiated; aluminum 2024-T3; corrosion properties

Introduction

Hybrid silica sol–gel organic–inorganic coatings deposited on AA2024-T3 have been extensively studied for their active properties to protect metals against the corrosion process.[1] The incorporation of non-hydrolyzable groups in conjunction with a different molar ratio of sol–gel precursors creates better protective barrier properties of the coatings. The sol–gel process has become an important synthesis route since its development offers new environmentally compliant chromate (VI)-free compounds that are based on the synthesis of an oxide network through inorganic polymerization when molecular precursors such as primary components are used. The development of hybrid sol–gels as compared with single inorganic oxide sol–gels has led to the improvement of corrosion resistance since brittleness and high curing temperatures have been averted.[2,3] Hybrid sol–gel coatings may be cured at temperatures below 200 °C, where the Si—O—Si or Me—O—Si network is formed.

In spite of these developments, hybrid sol–gel coatings still provide low corrosion resistances at longer immersion times since the sol–gel network forms superficial defects such as pores that weaken the protective properties of the coating. For this reason, different alternatives to enhance the corrosion resistance have been developed. The incorporation of particles such as clays, pigments or fibers mixed or stirred into the network may provide[4] better mechanical resistance of impact, scratch, wear as well as improvement in corrosion resistance. These additives may turn out to be controversial since the particles may react along with the network prior to the curing process, and some authors[5] do not support the corrosion resistance improvement. The hydrotalcite-like compound (HTLCs) is anionic clay that has shown an increment in coating resistance of the sol–gel coatings in saline media.[6] This enhancement is attributed to the lamellar structure of the HTLCs, which is capable of promoting an anionic exchange that captures the aggressive species of the media.[7,8]

On the other hand, it is widely known that the effect of gamma irradiation on structure, crystallization behavior and thermal properties of polymers induces structural changes in the network.[9–11] The irradiation effect will depend directly on the nature and features of the specific network as well as on the dose. The gamma-irradiated coatings reported in the literature describe mainly the electrical, thermal and mechanical properties. Since the information concerning corrosion performance is scarce and limited,[12] the irradiation of coatings with corrosion protection utility opens up other routes for enhancing the corrosion resistance. According to Bhattacharya,[13] the irradiation process offers many advantages over other conventional methods since no catalyst or additives are needed to initiate the reaction. The irradiation method is simple, and the degree of induced crosslinking is direct and controlled by the absorbed dose, which determines the extent of swelling in the hydrogels.[14]

* *Correspondence to: M. Hernandez, Dpto. de Materiales y Manufactura (CENISA) Facultad de Ingeniería, Universidad Nacional Autónoma de México, UNAM, Ciudad Universitaria, 04510 México, DF, México. E-mail: mahdz2010@comunidad.unam.mx*

† *Paper published as part of the ECASIA 2013 special issue.*

a *Dpto. de Ingeniería Metalúrgica, Facultad de Química, Universidad Nacional Autónoma de México, UNAM, Ciudad Universitaria, 04510 México, DF, México*

b *Dpto. de Materiales y Manufactura (CENISA) Facultad de Ingeniería, Universidad Nacional Autónoma de México, UNAM, Ciudad Universitaria, 04510 México, DF, México*

c *Dpto. Química de Radiaciones y Radioquímica. Instituto de Ciencias Nucleares, Universidad Nacional Autónoma de México, UNAM, Ciudad Universitaria, 04510 México, DF, México*

d *Instituto de Investigaciones en Materiales, Universidad Nacional Autónoma de México, UNAM, Ciudad Universitaria, 04510 México, DF, México*

The aim of the present paper is the study and characterization of gamma-irradiated hybrid sol–gel coatings doped with hydrotalcite (HT) and deposited on an aluminum AA2024-T3 alloy substrate.

Experimental program

The silica hybrid sol–gel solution was synthesized from a copolymerization of 3-glycydoxypropyltrimethoxysilane (GPTMS) as the organic precursor and tetra-n-propoxyzirconium (TPOZ) as the inorganic precursor. The organic sol was prepared by adding 2-propanol and GPTMS in conjunction with nitric acid of pH 0.5 as an acidic catalyst for 60 min. Simultaneously, the inorganic sol was prepared by combining ethylaceocetate and TPOZ under mechanical and ultrasonic stirring for 20 min followed by nitric acid of pH 0.5 for 90 min. Finally, both sols were mixed and stirred for 60 min in order to prepare the hybrid solution. Alternatively, synthetic hydrotalcite was used as received from Aldrich. Different HT weight percentages were used for doped sol–gel coatings: 5 and 10%, *w/w*. The nomenclature is as follows: undoped samples (no HT addition), SGO; 1% HT, SG1; and 5% HT, SG5.

AA2024-T3 samples were ground with silicon carbide paper, 240-grit, washed with distilled water and ultrasonically cleaned with ethanol. The sol–gel coatings were obtained by using the dip-coating method at a constant rate of 10 cm min^{-1} for 100 s of immersion. The curing temperature was 100 °C for 90 min.

Sol–gel solutions and cured sol–gel coatings were gamma irradiated by using a γ-source (Gammabeam 651 PT, MDS Nordion) in air and in vacuum at room temperature from 1 to 100 kGy. Both the sol–gel solutions and the cured coated samples were placed in glass ampoules. The samples irradiated in vacuum were first filled with argon to remove air and then sealed. The samples at atmospheric conditions were encapsulated and sealed.

In order to study and characterize the sol–gel coatings, differential scanning calorimetry (DSC) was employed using a DSC 2010 TA Instrument at a heating velocity of 10 °C min^{-1} with an argon stream at 80 ml min^{-1}. X-ray difrractograms were obtained using Brucker D8 Advance equipment with the monochromatized Cu, Kα of 1.5404 Å, from 2° up to 80°. FTIR spectra were obtained with a Perkin-Elmer Paragon 500 FTIR-ATR in the wavenumber range of 4000 to 700 cm^{-1}. Surface morphology was examined using scanning electron microscopy (SEM) and energy dispersive X-ray (EDX) with a DSC JEOL JSM-5900LV. Finally, in order to assess the corrosion performance, electrochemical impedance spectroscopy (EIS) was employed in an ACM Instrument using a sweeping frequency from 10 kHz down to 10 mHz with 10 points per decade at 10 mV of sinusoidal amplitude. All EIS measurements were performed in a NaCl 0.1 M solution at open circuit potential conditions. The electrochemical setup consisted of the working electrode (coated sample) of 1.39 cm^2, a saturated calomel electrode as a reference electrode and a graphite rod as a counter-electrode. At least two samples of each condition (vacuum and air) were tested in order to check reproducibility.

Results and discussion

According to impedance measurements of all irradiated systems including sol–gel solutions and coated samples either at atmospheric or vacuum conditions, the best dielectric properties were obtained for those coatings irradiated after the curing process. Figure 1 depicts the impedance diagrams obtained at the initial stage and after 144 h of testing. At the beginning of the test (initial stage), the EIS spectra show two time constants identified in all samples regardless of either the HT content or

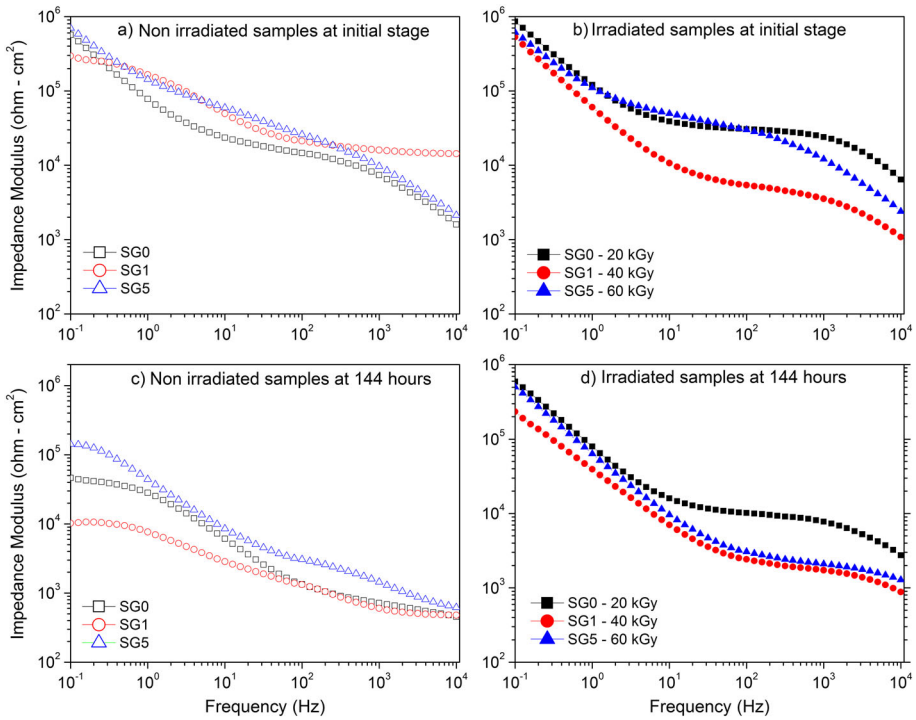

Figure 1. Impedance diagrams. Impedance modulus at initial stage of (a) non-irradiated samples and (b) irradiated samples. Impedance modulus at 144 h of testing of (c) non-irradiated samples and (d) irradiated samples.

the irradiated doses. However, at 144 h of immersion, the systems presented three different time constants.

At the initial stage, the first time constant in the range of kHz is ascribed to the dielectric properties of the sol–gel, whereas at the lower frequencies (below 1 Hz), the apparent time constant is related to the oxides/hydroxides present on the metal/coating interface. Nevertheless, at 144 h of immersion, the third constant belongs to the corrosion process of the metal substrate. In order to check the effect of the dose on the sol–gel network, the degree of porosity ($\rho_{NaCl(50\,\Omega cm)}/\rho_{sol-gel} \times 100$) obtained from EIS results for each system was calculated (Table 1). From these values, it is seen that SG0 and SG5 show similar degrees of porosity at the initial stage of immersion, whereas at 144 h of test, SG0 proves to be more effective as a protective coating according to the resistivity and porosity values, which are in agreement with the EIS spectra presented by Fig. 1b, where the SG0 (20 kGy) behavior of the Bode plot clearly indicates higher resistance values among all systems (mainly at low frequencies).

These results indicate that at higher hydrotalcite content the gamma-irradiated effect on the sol–gel network is blocked or absorbed since higher irradiated doses were needed in SG1 and SG5 in order to achieve a similar coating resistance to that presented by SG0. The positive effect on the dielectric properties of the sol–gel at 60 kGy at immersion time did not persist at 144 h; moreover, this high irradiation dose induced a higher degree of porosity on the sample at longer immersion times (Table 1). It should be borne in mind that the irradiation doses of 20 kGy, 40 kGy and 60 kGy for SG0, SG1 and SG5, respectively, were selected in accordance with previous results, i.e. all systems were irradiated from 1 to 100 kGy; afterwards, the samples were subjected to electrochemical impedance testing during 720 h with SEM assessment. It was observed that samples above 20 kGy for SG0, 40 kGy for SG1 and 60 kGy for SG5 of irradiation doses suffered surface deterioration (cracks) with very low coating resistance. For this reason, 20, 40 and 60 kGy represent the optimal irradiation dose for each system with the higher impedance in saline media.

The fact that SG0, SG1 and SG5 samples gave different coating thickness values after the curing process is due to the hydrotalcite content. In a previous publication,[1] it was shown that the incorporation of HT into the sol–gel coatings formed larger agglomerates as the HT content increases. For this reason, it is not possible to control or to set the same coating thickness throughout the systems. The incorporation of HT has a positive effect since the corrosion resistance of the aluminum increases but also induces defects such as pores due to agglomerates that affect the network reticulation. Therefore, in general, thicker coatings contain higher HT content that may induce more porosity with low resistivity. It is expected that thicker coatings will also show higher impedances (coating resistances) in a defect-free coating; however, as already mentioned, the size, the location and position of the HT agglomerates will affect the coating resistance.

On the other hand, comparing the EIS results of irradiated and non-irradiated samples, the immersion-irradiated SG0 gave better results in sol–gel resistance (Table 1) than those of doped samples. At 144 h of testing, the behavior did not change. The irradiated coatings of HT-containing samples exhibited lower dielectric properties and a higher degree of porosity compared with the irradiated sample with no hydrotalcite content. In other words, the γ-irradiation improves the corrosion resistance of the coated aluminum AA2024-T3 alloy without the incorporation of hydrotalcite. This improvement is also reflected in the low degree of porosity measured during the whole test. The fact that HT incorporation had an adverse impact on the corrosion protection will be analyzed in the following sections.

Figure 2 displays the FTIR spectra of all coated systems (SG0, SG1 and SG5) irradiated and non-irradiated. Different absorption peaks can be assigned along the spectra. The most significant are those identified as the OH in the stretching (3463 cm^{-1}) and bending (1635 cm^{-1}) mode, the vibration bands at 2935 and 2874 cm^{-1} associated with —C—H bonds and several bands of interlamellar carbonate species located at lower wavenumbers. A detailed explanation of these FTIR spectra is reported elsewhere.[1] As can be seen in Fig. 2, all FTIR spectra are similar except for high and low wavenumbers. The transmittance of the OH stretching mode and the carbonates species is lower as function of the γ-irradiation indicating that irradiation modifies

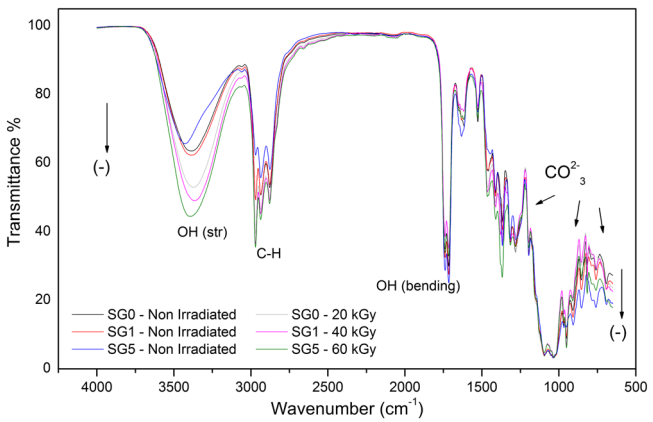

Figure 2. FTIR spectra of irradiated and non-irradiated samples of SG0, SG1 and SG5.

Table 1. Film parameters: thickness, coating resistance ($R_{sol-gel}$), coating resistivity ($\rho_{sol-gel} = R_{SG}/d$) and film porosity. These results are obtained at an initial stage and at 144 h of testing

Sample	Thickness μm	$R_{sol-gel—initial}$ (Ω-cm^2)	$\rho_{sol-gel—initial}$ (MΩ-cm)	Porosity (%) $\times 10^{-5}$	$R_{sol-gel—144\,h}$ (Ω-cm^2)	$\rho_{sol-gel—144\,h}$ (MΩ-cm)	Porosity (%) $\times 10^{-5}$
SG0—20	6.018	31 733	52.73	9.48	10 762	17.88	27.96
SG1—40	6.607	6080	9.2	54.34	2140	3.23	154.79
SG5—60	9.62	44 312	46	10.86	2568	2.66	187.9
SG0	5.5	18 994	34.53	14.44	5066	9.21	54.28
SG1	6.3	66 080	104.88	4.76	8534	13.54	36.92
SG5	8.72	63 703	73.05	6.84	6314	7.24	69.06

the entangled network obtained by the hydrolysis and polycondensation of metal alkoxides during the synthesis process. In accordance to FTIR and DSC results, it is established that irradiation promotes modification of the structural phase of the coatings that possibly reduces the OH bonds and the interactions of carbonates of the HT with the sol–gel that affects the densification of the sol–gel. Since transmittance is lower at higher γ-irradiation, this indicates that the film is more heterogeneous. By doping the sol–gel with higher HT content and higher γ-irradiation, the average transmittance of the films decreased.

Concerning the XRD patterns, Fig. 3 shows the diffractograms of the non-irradiated sample with no HT in conjunction with SG0 (20 kGy), SG1 (40 kGy) and SG5 (60 kGy). The XRD results reveal that non-irradiated and irradiated HT samples have a highly crystalline structure due to the hydrotalcite structure and the aluminum substrate. According to these spectra in conjunction with those observed by FTIR (Fig. 2), the functional groups of the HT were not affected by the γ-irradiation; however, it seems that the crystallite size was modified since the maximum length of the main peak at (003) of all HTs differed in each case as the doses increase (Fig. 3b). Therefore, the average crystal size was calculated in order to determine the effect of the irradiated dose. This calculation was carried out by using the Scherrer equation of the diffraction peaks (Fig. 3b), where $D_{h,k,l}$ is the average crystallite size of the (h k l) profile, λ is the wavelength of the incident X-rays (Cu, Kα, 0.15406 nm), $\beta_{h,k,l}$ is the full width at half-maximum of the (h k l) line and θ is the Bragg angle. The average sizes were as follows: non-irradiated HT—35.147 nm, irradiated SG0 (20 kGy)—40.41 nm, irradiated SG1 (40 kGy)—46.2 nm and irradiated SG5 (60 kGy)—52.1 nm.

The different gamma irradiation doses used in this research indicate that the hydrotalcite crystalline structure is not modified even at 60 kGy. These doses, 20, 40 and 60 kGy, promote the growth of the average crystallite size in the sol–gel network, which has a detrimental effect on the corrosion properties as compared with the non-irradiated samples in saline media. The maximum irradiation dose of 60 kGy was chosen because at this γ-irradiation, the doped sol–gel network had the best dielectric properties. Irradiated doses higher than 60 kGy had a negative effect on the corrosion properties of the doped coatings. However, in accordance with FTIR and X-ray results, this maximum level of irradiation did not affect the HT structure. It is known that the crystalline structure of HTLCs can be modified by microwave irradiation[15]; however, it seems that the hydrotalcite under γ-irradiation from 1 to 100 kGy does not suffer modification of the structural lattice. Therefore, it seems that the HT needs higher irradiation doses in order to modify the crystalline structure.

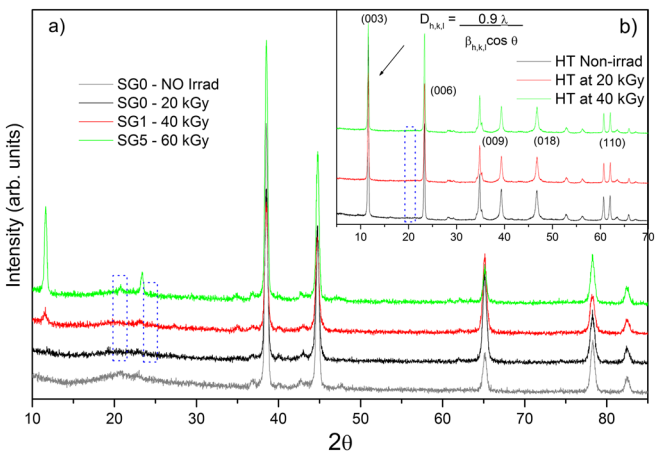

Figure 3. XRD patterns of non-irradiated sample (SG0) and irradiated samples (SG0, SG1 and SG5) (a); as well as non-irradiated hydrotalcite and irradiated hydrotalcite at 20 and 60 kGy (b).

Martinez-Gallegos *et al.*[16] have irradiated hydrotalcite at doses at around 6 MGy, where a significant change in the crystalline orientation was obtained. It is feasible to think that irradiating doses in HT in the magnitude of MGy could also promote a larger crystallite size; however, larger HT particles also affected the corrosion performance. In previous publications[1,6], it has been demonstrated that HT tends to form larger agglomerates with heterogeneous dispersion in the sol–gel network, which reduces the dielectric properties of the coating. If the hydrotalcite crystallite size becomes larger, the corrosion properties will probably decrease even further.

In addition, it is observed from Fig. 3 that another contribution in the range of 20.787 and 27.312 of 2θ can be identified. The peaks observed in these bands grow slowly as a function of the dose. For higher hydrotalcite doses of the order of MGy, these peaks indicate a possible preferential crystallinity orientation of the hydrotalcite as reported in literature.[16] These peaks do not belong either to the reflection of the tetragonal zirconia (GPTMS + TPOZ as precursors) or the aluminum substrate.

Concerning the DSC results of non-irradiated samples, Fig. 4a displays the thermograms of SG0, SG1 and SG5 samples. Two endothermic regions below 100 °C are clearly distinguished (region I). The first peak around 43 °C and the second peak (83.5 °C) are ascribed to evaporation of organic compounds as well as removal of water by evaporation.[17,18] The second region located around 145 °C is probably attributed to glass transition temperature (Tg) of the sol–gel since the shape of the curve is typical of the *Tg* behavior of a polymer-base coating. This transition temperature becomes more evident at higher hydrotalcite content (HT5). The third region (exothermic peak) around 358 °C is associated with decomposition of the sol–gel coating.

In order to corroborate the participation of the HT in the thermal properties of the sol–gel, the hydrotalcite thermogram is also compared with the sol–gel coatings. As can be seen in Fig. 2, the HT transitions do not participate in the sol–gel transitions. The first hydrotalcite peak presents at 281 °C, which corresponds to the beginning of the detection of the change in heat flow of decomposition of sol–gel. Therefore, in accordance with Fig. 2, the incorporation of HT into the sol–gel clearly modifies the thermal behavior of the coating. The evaporation temperatures and the glass transition temperatures (*Tg*) are increased at higher HT content.

On the other hand, the irradiated samples shown in Fig. 4b also depict modification of the thermal properties of the sol–gel as function of dose. In region I, related to evaporation of solvents, samples suffer an increment of the transition temperatures whereas the water molecule temperature removal remains unchanged. However, region II exhibits the main effect of the γ-irradiation where the zone ascribed to glass transition temperature increases its temperature value as function of the γ-dose, which means that at higher dose the amorphous character of the coatings likely becomes more rigid in the final network. The decomposition temperature of the doped coatings also increases at the same value of 362 °C regardless of the HT content or the γ-dose.

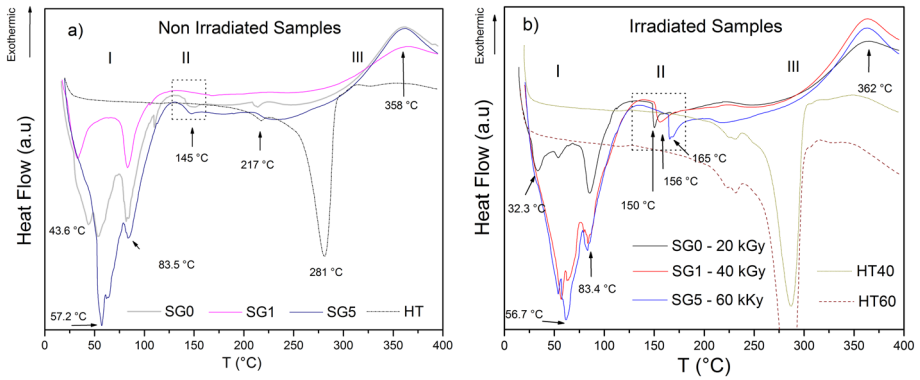

Figure 4. DSC thermograms of (a) non-irradiated and (b) irradiated samples.

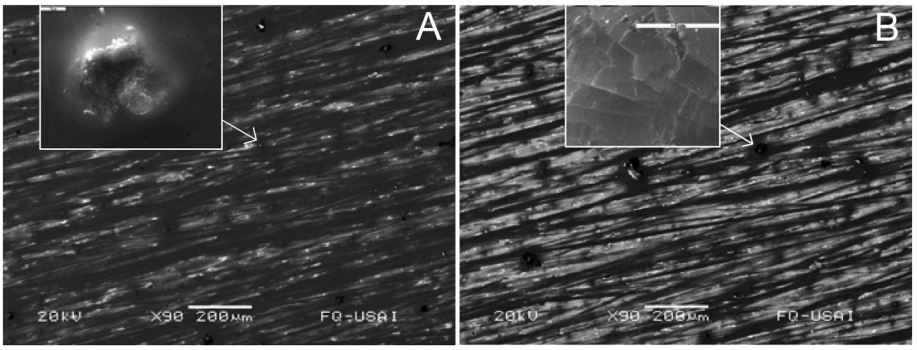

Figure 5. SEM micrographs of (a) non-irradiated SG5 and (b) irradiated SG5 at 90×.

Finally, the hydrotalcite thermograms with 40 and 60 kGy reveal that the main effect of the irradiation consists in separating the first transitions of interlayer water into two small peaks at 224 °C and 231 °C. This behavior induces one to think that the hydrotalcite particles would probably separate their crystal lattice that allowed the removal of water molecules at different superficial interlayer depths.

Therefore, in accordance to all results of Fig. 2, the thermal transitions of doped sol–gel coatings with and without irradiation are completely different from those obtained with pure hydrotalcite which means that the transitions presented in the thermograms of SG1 and SG5 are related to the combination and interactions of the sol–gel with the hydrotalcite particles.

Regarding the superficial topography, different analyses using SEM/EDX were carried out. Figure 5 depicts the SEM micrograph of irradiated and non-irradiated samples doped with 5% HT. An average particle size of 20 µm was found over the whole surface with heterogeneous dispersion, i.e. random distribution of aggregates and isolates particles onto the coated surface. Particles below 5 µm in size were also detected. The main feature of irradiated samples is that the HT particles are more visible and the defects are bigger compared with non-irradiated conditions. A closer look at the particles reveals that irradiated HT shows superficial scratches whereas the non-irradiated HT shows a homogeneous surface. These analyses support the EIS and the X-ray results. The growth of the HT as a consequence of the radiation process also contributes to the degradation of the sol–gel coating and the increase of the superficial defects, such as pores or scratches that decreased the corrosion protection of the coating.

Conclusions

Hybrid silica sol–gel coatings were synthesized from organic and inorganic precursors. These coatings were doped with synthetic hydrotalcite. This procedure demonstrates better corrosion protection in saline media. However, when these HT-doped coatings were irradiated at 40 and 60 kGy, their barrier properties notably decreased as compared with the case of undoped HT coatings. A positive effect of γ-irradiation was achieved for sol–gel coatings without the incorporation of hydrotalcite at 20 kGy, which improves the corrosion resistance of coated aluminum AA2024-T3. The irradiated hydrotalcite evidenced a crystallite growth that damages the sol–gel network, creating more superficial defects such as pores and scratches. This damage may be also induced by the structure of the coating that slowly evolves to a more amorphous and heterogeneous network as the dose increases.

Acknowledgements

This research has been supported by the Consejo Nacional de Ciencia y Tecnología Project 167856. Authors also acknowledge support from DGAPA (Dirección General de Asuntos del Personal Académico) through PAPIIT program IB100112 and Programa de Becas Posdoctorales of Alba Covelo Villar from Universidad Nacional Autónoma de México 2013–2014, México.

References

[1] D. Álvarez, A. Collazo, M. Hernández, X. R. Nóvoa, C. Pérez, *Prog. Org. Coat.* **2010**, *67*, 152.

[2] Y. Joshua Du, M. Damron, G. Tang, H. Zheng, C.-J. Chu, J. H. Osborne, *Prog. Org. Coat.* **2001**, *41*, 226.
[3] A. J. Vreugdenhil, V. N. Balbyshee, M. S. Donley, *J. Coating Tech.* **2001**, *73*, 35.
[4] J. D. Mackenzie, *J. Sol-gel Sci. Tech.* **1994**, *2*, 81.
[5] N. N. Voevodin, N. T. Grebasch, W. S. Soto, F. E. Arnold, D. S. Donley, *Surf. Coat. Technol.* **2001**, *140*, 24.
[6] A. Collazo, M. Hernandez, X. R. Nóvoa, C. Pérez, *Electrochim. Acta* **2011**, *56*, 7805.
[7] R. G. Buchheit, H. Guan, S. Mahajanam, F. Wong, *Prog. Org. Coat.* **2003**, *47*, 174.
[8] G. Williams, H. N. McMurray, *Electrochem. Solid State Lett.* **2004**, *7*, B13.
[9] T. Yovcheva, M. Marudova, A. Viraneva, E. Gencheva, N. Balanov, G. Mekishev, *J. Appl. Polymer Sci.* **2013**, DOI: 10.1002/APP.38140.
[10] F. Djouani, Y. Zahra, B. Fayolle, M. Kuntz, J. Verdu, *Radiat. Phys. Chem.* **2013**, *82*, 54.
[11] Y. Liu, C. Luo, Z. Ye, X. Yuan, D. Yang, 9th International Conference on Protection of Materials and Structures From Space Environment, ICPMSE-9, Toronto, Canada, **2008**.
[12] R. David, S. P. Tambe, S. K. Singh, V. S. Raja, D. Kumar, *Surf. Coating Tech.* **2011**, *205*, 5470.
[13] A. Bhattacharya, *Prog. Polym. Sci.* **2000**, *25*, 371.
[14] E. Jabbari, S. Nozari, *Eur. Polym. J.* **2000**, *36*, 2685.
[15] G. Negrón, L. Soto, A. Guerra, L. Lomas, J. Mendez, *Rev. Soc. Quin. Méx.* **2000**, *44*, 251.
[16] S. Martinez-Gallegos, S. Bulbulian, *Clay Clay Miner.* **2004**, *52*, 650.
[17] D. H. Aguilar, L. C. Torres-González, L. M. Torres-Martínez, T. López, P. Quintana, *J. Solid State Chem.* **2000**, *158*, 349.
[18] F. Rubio, J. Rubio, J. L. Otero, *Thermochim. Acta***1998**, *320*, 231.